

Transition from the cholesteric storage mode to the nematic phase in critical restricted geometries

Marshall Luban

*Department of Physics, Bar-Ilan University, Ramat-Gan, Israel
and Department of Electronics, Weizmann Institute of Science, Rehovot, Israel*

David Mukamel*

*Department of Electronics, Weizmann Institute of Science, Rehovot, Israel
and Nuclear Research Center-Negev, P.O. Box 9001, Beer Sheva, Israel*

Shmuel Shtrikman

Department of Electronics, Weizmann Institute of Science, Rehovot, Israel

(Received 20 February 1974)

It is shown that a cholesteric liquid crystal, between parallel confining plates of spacing $2L$, prepared in the "storage mode" (helix axis parallel to plates) undergoes a transition to the nematic state when L is decreased to a critical value L_c . For $0 < (L - L_c)/L_c \ll 1$ the pitch of the cholesteric helix diverges as $\ln(L - L_c)$.

I. INTRODUCTION

Cholesteric liquid crystals are currently under intensive investigation with emphasis placed on both their basic physical properties as well as their possible utilization in device applications. A common experimental arrangement is where the cholesteric is confined between two parallel plates tending to align the director parallel to the plates. For this geometry the stable configuration occurs when the axis of the helical structure lies perpendicular to the confining plates. Recently experimentalists have succeeded in preparing a long-lived configuration where the axis lies parallel to the plates.¹⁻³ This configuration, because of its long lifetime, is of considerable interest as regards possible storage applications. We propose the name "storage mode" for this configuration. In the present work we develop a theory for a model storage-mode cholesteric system.

We consider the model system of a cholesteric liquid crystal prepared in the storage mode which is confined between two infinite parallel plates with spacing $2L$. It is to be expected that the surface energy of interaction per unit area between the cholesteric and the plates can be written as $(C/2)f(\Phi)$, where f is a periodic function of the angle Φ between the director and the plates, with period π (see Fig. 1). Furthermore, the function is expected to have a single minimum, say at $\Phi=0$, in the fundamental interval $-\frac{1}{2}\pi < \Phi < \frac{1}{2}\pi$ and to be a symmetric function about the minimum. The mathematical calculations are rendered tractable by adopting the simplest choice compatible with these requirements, $f(\Phi) = \Phi^2$ for

$-\frac{1}{2}\pi < \Phi < \frac{1}{2}\pi$ and $f(\Phi + \pi) = f(\Phi)$ (see Fig. 2). We obtain the spatial dependence of the director as well as the pitch of the helix as functions of both the plate spacing $2L$ and the surface-energy coefficient C . In particular, we find that as L is decreased to a critical value L_c the pitch diverges logarithmically when $L - L_c$ approaches zero, and thus the system is nematic for $L \leq L_c$. This result is reminiscent of the de Gennes calculation⁴ which showed that in the presence of a magnetic field applied perpendicularly to the helix axis of bulk cholesteric, the pitch diverges logarithmically with $H_c - H$ as H is increased to the critical field H_c . We also note that the present result, giving the pitch as a function of $L - L_c$ as well as the surface-energy coefficient C suggests that measurements of this quantity close to critical spacing might serve to fix C .⁵

In Sec. II we present the basic equations which describe the system under investigation. Minimization of the total free energy leads to a differential equation for the director as well as the appropriate boundary conditions. We establish the equilibrium behavior of the director and the pitch of the helical structure as functions of L and C , as well as the dependence of the critical spacing L_c on C .

In Sec. III we summarize our main conclusions as well as provide some numerical estimates of relevance to an experimental confirmation of the storage mode to nematic phase transition.

In Appendix A we consider bulk cholesteric in an external magnetic field applied perpendicular to the helix axis. The magnetic energy is chosen proportional to $H^2 f(\Phi)$ where $f(\Phi)$ is the same periodic function adopted in Sec. II [Eq. (2.8)] for

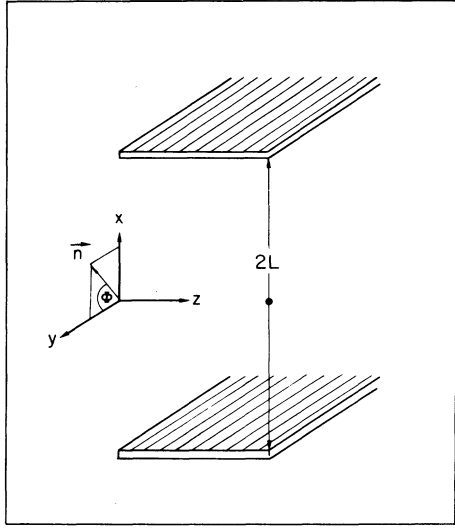


FIG. 1. Schematic diagram of the geometry of the two parallel infinite plates separated by a distance $2L$. The director of the cholesteric is assumed to lie in the xy plane.

the surface energy. The results are found to be in close numerical agreement with those of de Gennes⁴ obtained for the physically more reasonable choice $f(\Phi) = \sin^2\Phi$. Our choice for $f(\Phi)$ and $\sin^2\Phi$ share the common property of being periodic functions with a single minimum in any interval of length π and symmetric about their minimum. The close numerical agreement between the results obtained using these two functions leads us to conclude more generally that the qualitative nature of our results in the main text will be the same for a wide class of periodic functions $f(\Phi)$ with the aforementioned properties.

II. BASIC EQUATIONS

We consider an infinite slab of cholesteric liquid crystal confined between two parallel plates separated by a distance $2L$. We assume a surface interaction which at the plate faces constrains the director to lie only in the xy plane and favors

alignment in the y direction (see Fig. 1). (Experimentally this could be achieved by suitable rubbing of the plates in the y direction.) In the present work our attention is confined to the cholesteric storage mode and for this mode we assume that at any point between the plates the director lies only in the xy plane, $\hat{n} = n_x \hat{i} + n_y \hat{j}$. If Φ denotes the angle between the director and the y axis, we assume that Φ depends only upon x and z ,

$$n_x = \sin\Phi(x, z), \quad n_y = \cos\Phi(x, z). \quad (2.1)$$

As discussed in the Introduction, it is reasonable to suppose that the surface free energy per unit area can be written as $(C/2)f(\Phi(\pm L, z))$ where $f(\Phi)$ is a periodic function with period π , since the directors $\pm\hat{n}$ correspond to the same physical state. Without loss of generality we can choose C to be positive, and $f(\Phi)$ is then expected to have a single minimum, chosen as $\Phi = 0$, in the fundamental interval $-\frac{1}{2}\pi < \Phi < \frac{1}{2}\pi$ and to be an even function of Φ . The total free energy of the system is given by the sum of the Frank free-energy expression and the surface free energy. To simplify the treatment, we consider the so-called isotropic case whereby the three Frank constants K_{11}, K_{22}, K_{33} are equal. Also in the present treatment we exclude the possibility of disclinations.

One can anticipate that for the equilibrium situation the cholesteric ordering is such that the director traces out a *periodic* helix as a function of z . Denoting the pitch of the helix by 2λ , the angle Φ changes by π as z increases by an amount λ ,

$$\Phi(x, z + \lambda) = \pi + \Phi(x, z). \quad (2.2)$$

With these assumptions the total free energy per unit volume can be written as

$$F = \frac{1}{2L\lambda} \int_{-L}^L dx \int_{-\lambda/2}^{\lambda/2} dz \times \left\{ \frac{1}{2} K_{11} \left[\left(\frac{\partial \Phi}{\partial x} \right)^2 + \left(\frac{\partial \Phi}{\partial z} \right)^2 \right] - K_{11} q_0 \frac{\partial \Phi}{\partial z} + \frac{1}{2} C f(\Phi) [\delta(x-L) + \delta(x+L)] \right\}. \quad (2.3)$$

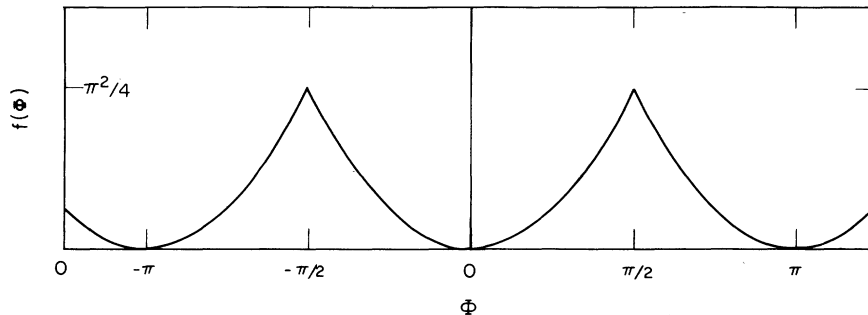


FIG. 2. Periodic function $f(\Phi) = \Phi^2$, $-\frac{1}{2}\pi < \Phi < \frac{1}{2}\pi$; $f(\Phi + \pi) = f(\Phi)$ of Eq. (2.8).

The integration over x is understood to extend from $-(L+0)$ to $+(L+0)$ in order that $\int_{-L}^L dx \delta(x \pm L) = 1$. It is further understood that the derivatives $\partial\Phi/\partial x$ and $\partial\Phi/\partial z$ are continuous functions of x and z , for otherwise Eq. (2.3) will fail to describe the correct free energy per unit volume. This requirement further ensures the existence of the second derivatives appearing below in the Euler equation (2.4). The choice of sign of the term $K_{11}q_0(\partial\Phi/\partial z)$ is such that for bulk cholesteric the equilibrium director traces out a left-handed helix, and $2\pi/q_0$ denotes the pitch in that case.

The equilibrium form of $\Phi(x, z)$ is obtained by minimizing the functional of Eq. (2.3). The corresponding Euler equation is given by

$$K_{11}\nabla^2\Phi - \frac{1}{2}Cf'(\Phi)[\delta(x-L) + \delta(x+L)] = 0. \quad (2.4)$$

Equivalently, for $-L < x < L$, Eq. (2.4) reduces to Laplace's equation, while for $x = \pm L$,

$$\mp K_{11}\frac{\partial\Phi}{\partial x}(\pm L, z) - \frac{1}{2}Cf'(\Phi(\pm L, z)) = 0. \quad (2.5)$$

We assume that, among the solutions of Eqs. (2.4) and (2.5) satisfying Eq. (2.2), the state of lowest free energy provides a local minimum, or at worst a saddle point, for the free-energy functional.

The requirement of Eq. (2.2) is satisfied if

$$\Phi(x, z) = qz + \phi(x, z), \quad (2.6)$$

where ϕ is a periodic function of z with period λ , and $q = \pi/\lambda$. Although the surface energy and the bulk Frank free energy generally compete against each other, the one seeking to maintain the molecules parallel to the plates and the other seeking to maintain $\Phi = qz$, they both allow the planes $z = n\lambda$ to be planes of constant $\Phi = n\pi$. This property is incorporated by restricting $\Phi(x, z)$ to be an odd function of z , in addition to Eq. (2.6). Also, in view of the symmetric geometry, we require Φ to be an even function of x . The solution of Laplace's equation which is periodic in z with period λ and which is even in x and odd in z is

$$\phi(x, z) = \sum_{n=1}^{\infty} A_n \cosh(2nqx) \sin(2nqz). \quad (2.7)$$

The program consists first of obtaining the expansion coefficients A_n for a given value of q so as to satisfy Eq. (2.5) and then of calculating the corresponding free energy F of Eq. (2.3). The equilibrium value \bar{q} is found by minimizing the resulting value of F as a function of q . Our interest lies in studying the spatial dependence of the equilibrium director as well as \bar{q} as a function of the variable plate spacing. Experimentally, these quantities can be ascertained by optical

measurements. In general, the ensuing calculations prove to be extremely formidable because Φ appears in Eq. (2.5) nonlinearly. To avoid this difficulty, in the present work we shall restrict our attention to the following simple choice for f (see Fig. 2),

$$\begin{aligned} f(\Phi) &= \Phi^2, \quad -\frac{1}{2}\pi < \Phi < \frac{1}{2}\pi, \\ f(\Phi + \pi) &= f(\Phi). \end{aligned} \quad (2.8)$$

Equation (2.5) is thereby replaced by

$$\mp K_{11}\frac{\partial\Phi}{\partial x}(\pm L, z) - Cqz - C\phi(\pm L, z) = 0, \quad -\frac{1}{2}\lambda < z < \frac{1}{2}\lambda. \quad (2.9)$$

To obtain the coefficients A_n appearing in Eq. (2.7) we utilize the Fourier-series expansion

$$z = \frac{\lambda}{\pi} \sum_{n=1}^{\infty} \frac{(-1)^{n+1}}{n} \sin\left(\frac{2\pi n z}{\lambda}\right) \quad (2.10)$$

for the relevant range $-\frac{1}{2}\lambda < z < \frac{1}{2}\lambda$. In this way one obtains the result

$$A_n = \frac{(-1)^n C}{n} \left[\frac{2\pi K_{11}}{\lambda} n \sinh\left(\frac{2\pi n L}{\lambda}\right) + C \cosh\left(\frac{2\pi n L}{\lambda}\right) \right]^{-1}. \quad (2.11)$$

Substituting for A_n in Eq. (2.7) and recalling Eq. (2.1), gives the director at each point within the cholesteric. It is then straightforward, although tedious, to show that the free energy, Eq. (2.3) in conjunction with Eq. (2.8), expressed in units of $K_{11}q_0^2$, is given by

$$F(Q, l) = \frac{1}{2}Q^2 - Q + (Q/l)S(Q, l), \quad (2.12)$$

where

$$S(Q, l) = \sum_{n=1}^{\infty} \frac{1}{n} \frac{\tanh(nQl)}{1 + n(Q/c)\tanh(nQl)}, \quad (2.13)$$

and the dimensionless quantities Q , l , and c are defined by $q = q_0 Q$, $l = 2q_0 L$, $c = C(2K_{11}q_0)^{-1}$.

The next step consists of minimizing $F(Q, l)$ as a function of Q for given values of l and c . This of course requires a knowledge of the Q dependence of the infinite series $S(Q, l)$. First note that for $Ql \geq 4$ each of the functions $\tanh(nQl)$ can be replaced by unity and thus

$$S(Q, l) \sim \gamma + \psi(1 + c/Q), \quad (2.14)$$

where $\gamma = 0.5772156\dots$ is Euler's constant and $\psi(z) = \Gamma'(z)/\Gamma(z)$ is the ψ or di-gamma function. Secondly, in Appendix B we employ the Poisson summation formula in order to express $S(Q, l)$ as the following expansion, which is particularly useful when $Ql \lesssim 1$,

$$S(Q, l) = A(c/l) - \frac{1}{2}Ql + 2\pi(c/l)^2 \sum_{m=1}^{\infty} y_m^{-1} [\exp(2\pi y_m/Ql) - 1]^{-1} [c/l + (c/l)^2 + y_m^2]^{-1}. \quad (2.15)$$

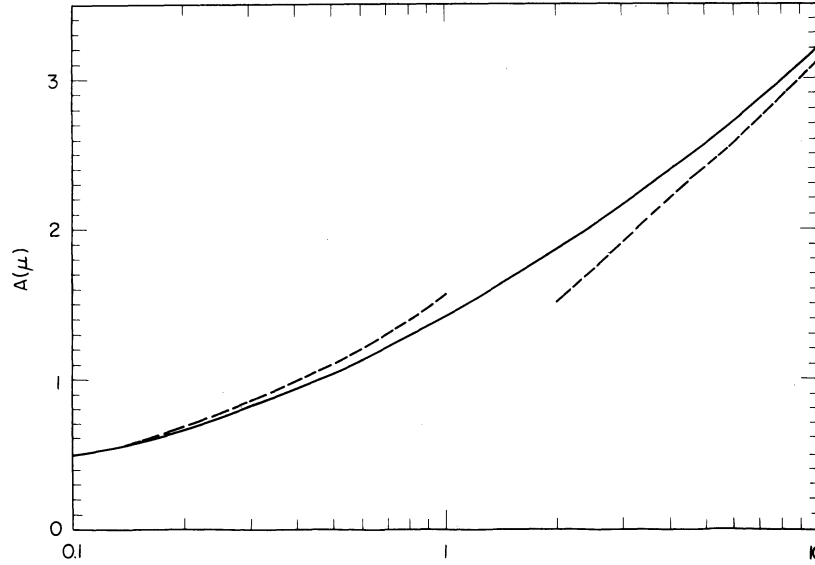


FIG. 3. Solid curve is a plot of the function $A(\mu)$ defined in Eq. (2.16) of the text. The dashed curves describe the limiting forms, $\frac{1}{2}\pi\mu^{1/2}$ and $\ln\mu + \gamma + \ln(4/\pi)$, which can be used for $\mu \lesssim 0.1$ and $\mu \gtrsim 10$, respectively.

Here

$$A(\mu) = \int_0^\infty dx \frac{\tanh x}{x[1 + (x/\mu)\tanh x]} \quad (2.16)$$

and y_m ($m=1, 2, \dots$) are the positive, real roots of

$$y_m \tanh y_m = \mathcal{C}l, \quad (2.17)$$

ordered so that $y_{m+1} > y_m$. As shown in Appendix B, the limiting behavior of $A(\mu)$ is $A(\mu) \sim \frac{1}{2}\pi\mu^{1/2}$ for $\mu \ll 1$ and $A(\mu) \sim \ln\mu + \gamma + \ln(4/\pi)$ for $\mu \gg 1$. In Fig. 3 a plot of this function is given. We also note that the following approximate analytic expression differs from $A(\mu)$ by less than 1%⁶ for all μ ,

$$A_{\text{approx}}(\mu) = \ln(1 + \frac{1}{2}\mu) + 2(1 + 4/\mu)^{-1/2} \times \tan^{-1}(1 + 4/\mu)^{1/2}. \quad (2.18)$$

We are now in a position to obtain $\bar{Q}(l, \mathcal{C})$, the value of Q which minimizes $F(Q, l)$. Note first that if the plates are very far apart ($l \gg 1$), using Eqs. (2.12) and (2.14) one has

$$\bar{Q}(l, \mathcal{C}) = 1 - l^{-1}[\gamma + \psi(\mathcal{C}) - \mathcal{C}\psi'(\mathcal{C}) + 2/\mathcal{C}] + O(l^{-2}). \quad (2.19)$$

Thus the system is cholesteric and \bar{Q} differs but slightly from its value for the bulk case. Second, we remark on the behavior of $F(Q, l)$ for small Q but for arbitrary plate spacing. As long as $Ql \lesssim 1$, F is very accurately given by discarding all terms but the first of the infinite series in Eq. (2.15), that is,

$$F(Q, l) = -[1 - l^{-1}A(\mathcal{C}l)]Q + 2\pi\mathcal{C}^2 l y_1^{-1} Q \times \frac{1}{e^{2\pi y_1/Ql} - 1} \frac{1}{y_1^2 + \mathcal{C}l + (\mathcal{C}l)^2}. \quad (2.20)$$

Now the factor $1 - l^{-1}A(\mathcal{C}l)$ is positive as long as l is larger than some value l_c , and negative for $l < l_c$. Thus as long as $1 - l^{-1}A(\mathcal{C}l) > 0$, corresponding to $l > l_c$, it follows that F has negative slope for smallest Q values. The free energy will therefore possess a negative minimum value for some positive definite value \bar{Q} and the system continues to be cholesteric. However, once l is decreased below l_c the quantity $1 - l^{-1}A(\mathcal{C}l)$ is negative, with the consequence that the minimum value of F is zero, and this occurs for $\bar{Q} = 0$, corresponding to the system being nematic. That is, a transition from the cholesteric to the nematic state occurs for the critical plate spacing l_c , satisfying the equation

$$A(\mathcal{C}l_c) = l_c. \quad (2.21)$$

A plot of l_c vs \mathcal{C} is given in Fig. 4. In Fig. 5 are shown a set of typical curves of $F(Q, l)$ vs Q for plate spacings with $l > l_c$, $l = l_c$, and $l < l_c$. Finally, in Fig. 6 are shown curves for $1/\bar{Q}(l, \mathcal{C})$ as a function of l for several values of \mathcal{C} .

We now obtain an analytic expression for $\bar{Q}(l, \mathcal{C})$ for values of l slightly larger than the critical value l_c . In this regime $\bar{Q}(l, \mathcal{C})$ is of course very small and one can employ Eq. (2.20) for the purpose of establishing the minimum of $F(Q, l)$. It is then straightforward to show that for $0 < (l - l_c)/l_c \ll 1$

$$\bar{Q}(l, \mathcal{C}) \sim -2\pi\left(\frac{y_1}{l_c}\right) \frac{1}{\ln(l - l_c)}. \quad (2.22)$$

This result is analogous to the result⁴ of de Gennes for the case of the bulk cholesteric in magnetic fields just below the critical field.

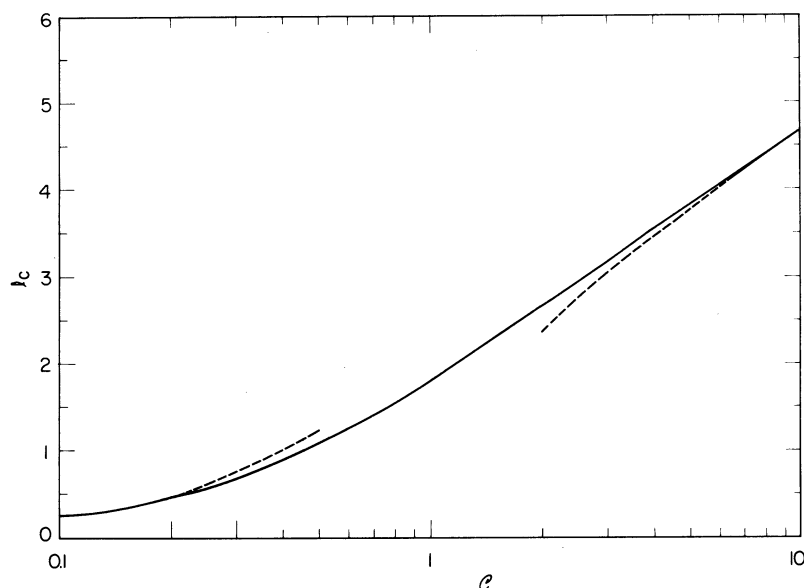


FIG. 4. Solid curve is a plot of the critical spacing parameter l_c vs C , obtained by solving Eq. (2.21). The dashed curves correspond to replacing $A(\mu)$ in Eq. (2.21) by the limiting forms $\frac{1}{2}\pi\mu^{1/2}$ and $\ln\mu + \gamma + \ln(4/\pi)$ appropriate for small and large values of μ , respectively.

III. DISCUSSION

In this work we have developed a simple model for the cholesteric storage mode. We have found that as the plate spacing is decreased to a critical value the system becomes nematic. Furthermore, we have obtained (see Fig. 4) the critical spacing as a function of the relevant parameters of the model, including K_{11} , the pitch $\lambda_0 = \pi/q_0$ of the bulk

cholesteric, and the surface-energy coefficient C . Finally, we have determined both the equilibrium pitch of the cholesteric helix and the spatial dependence of the director for variable plate spacing. In the vicinity of the critical spacing we have found that the pitch diverges proportional to $\ln(L - L_c)$.

It would be of considerable interest if the pre-

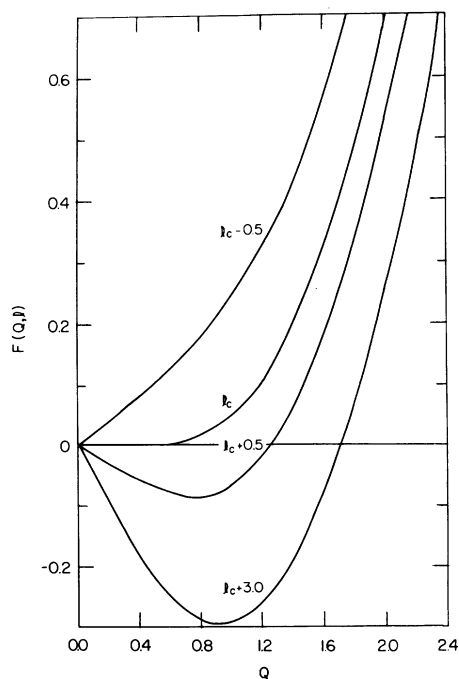


FIG. 5. Plot of the free energy $F(Q, l)$ of Eq. (2.12) vs Q for $l = l_c - 0.5$, l_c , $l_c + 0.5$, and $l_c + 3.0$ for the case $C = 1$.

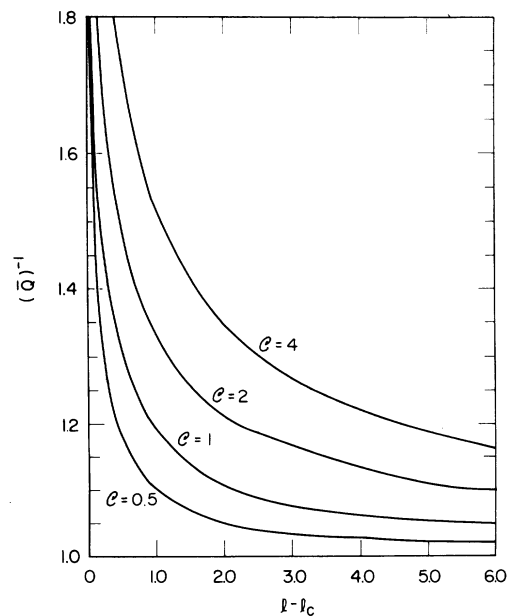


FIG. 6. Plot of the equilibrium pitch, in units of the equilibrium pitch for bulk cholesteric, vs $l - l_c$ for $C = 0.5, 1.0, 2.0$, and 4.0 . For large values of $l - l_c$ this quantity extrapolates to unity, whereas for $l - l_c$ tending to zero it diverges logarithmically [see Eq. (2.22)].

dicted transition of the cholesteric storage mode to the nematic phase could be put to an early experimental test. The following rough estimate suggests that the experiment is in fact feasible. The critical plate spacing $l_c = 2\pi L_c / \lambda_0$ is shown in Fig. 4 as a function of $\mathcal{C} = \lambda_0 C (2\pi K_{11})^{-1}$. Now typically $K_{11} \sim 10^{-6}$ dyn, and if for C we adopt the estimate⁷ of 1 erg/cm² and suppose that $\lambda_0 \sim 10 \mu$ one obtains $\mathcal{C} \sim 160$ and thus $L_c \sim 13 \mu$.

ACKNOWLEDGMENTS

We are grateful to Dr. E. Beller for several profitable discussions regarding the infinite series of Eq. (2.13), and to D. Lieberman for performing several calculations using the computer facilities of the Bar-Ilan University computation center.

APPENDIX A

The free energy per unit volume of the bulk cholesteric in the presence of a magnetic field normal to the axis of the helix is chosen by de Gennes⁴ to be of the form

$$F = \frac{1}{\lambda} \int_{-\lambda/2}^{\lambda/2} dz \left[\frac{1}{2} K_{22} \left(\frac{\partial \Phi}{\partial z} \right)^2 - K_{22} q_0 \frac{\partial \Phi}{\partial z} + \frac{1}{2} \chi_a H^2 \sin^2 \Phi \right]. \quad (\text{A1})$$

The main results of the calculation of de Gennes are as follows. The period of the spiral $\lambda(H)$ satisfies the equation

$$\lambda(H)/\lambda_0 = (2/\pi)^2 K(\xi) E(\xi), \quad (\text{A2})$$

where $\lambda_0 = \lambda(H=0) = \pi/q_0$, and K and E are the usual complete elliptic integrals of the first and second kind, respectively.⁸ The parameter ξ is defined implicitly by the equation

$$H/H_c = \xi/E(\xi), \quad (\text{A3})$$

where H_c denotes a critical magnetic field defined by

$$H_c = \frac{\pi}{2} \left(\frac{K_{22}}{\chi_a} \right)^{1/2} q_0. \quad (\text{A4})$$

When H is increased to H_c the system undergoes a transition to the nematic state as evidenced by the fact that, according to Eqs. (A3) and (A4), $\xi \rightarrow 1$ and $\lambda(H)$ diverges in this limit. In the immediate vicinity of H_c , $\lambda(H) \propto -\ln(H_c - H)$, whereas for weak fields $\lambda(H)/\lambda_0 = 1 + O(H^4)$.

We shall now show that the same qualitative behavior results if the magnetic energy term $\frac{1}{2} \chi_a H^2 \sin^2 \Phi$ is replaced by $\frac{1}{2} A \chi_a H^2 f(\Phi)$, where $f(\Phi)$ is given by Eq. (2.8) and A is a numerical coefficient which will be fixed in the following. The relevant Euler equation corresponding to

this modification is given by

$$K_{22} \ddot{\Phi}(z) - A \chi_a H^2 \Phi(z) = 0 \quad (-\frac{1}{2}\lambda < z < \frac{1}{2}\lambda), \quad (\text{A5})$$

and Φ is subject to the boundary conditions $\Phi(\pm \frac{1}{2}\lambda) = \pm \frac{1}{2}\pi$. The appropriate solution of Eq. (A5) is given by

$$\Phi(z) = \frac{\pi}{2} \frac{\sinh[(2h/Q)(2z/\lambda)]}{\sinh(2h/Q)} \quad (-\frac{1}{2}\lambda < z < \frac{1}{2}\lambda), \quad (\text{A6})$$

where $Q = q/q_0$, $q = \pi/\lambda$, $h = H/H_c$, and the magnetic field H_c is defined by

$$H_c = \frac{4}{\pi} \left(\frac{K_{22}}{A \chi_a} \right)^{1/2} q_0. \quad (\text{A7})$$

Evaluation of the free energy is straightforward with the result

$$F(Q) = K_{22} q_0^2 Q \left[-1 + h \coth \left(\frac{2h}{Q} \right) \right]. \quad (\text{A8})$$

For small values of Q the leading contribution to F is linear in Q and with slope $-1 + h \operatorname{sgn} Q$. Thus as long as $h < 1$ the minimum free energy occurs for nonzero values of Q and the system is cholesteric. However, for $h > 1$ the minimum free energy occurs for $Q = 0$, corresponding to the nematic phase. The present result for H_c , Eq. (A7), differs from the result of de Gennes [Eq. (A4)] by a factor $8\pi^{-2} A^{-1/2}$. We shall in fact choose $A = 64\pi^{-4}$ so that our result for H_c will agree with that of de Gennes.

We now calculate $\bar{Q}(h)$, the minimizing value of Q , for magnetic fields just below H_c , and we show that $\bar{Q}(h) \sim -1/\ln(1-h)$, the same functional dependence as found by de Gennes. The calculation is performed utilizing the fact that \bar{Q} is extremely small when $h \lesssim 1$. Thus one can approximate the hyperbolic cotangent function in Eq. (A8) by $1 + 2e^{-(4h/Q)}$, so that in this approximation

$$F(Q) \approx K_{22} q_0^2 Q [-1 + h(1 + 2e^{-4h/Q})]. \quad (\text{A9})$$

Minimizing F vs Q leads directly to the result

$$\bar{Q}(h) \sim -4h/\ln(1-h). \quad (\text{A10})$$

It will be noted that the specific value of A does not enter explicitly in this result. By contrast, for $h \lesssim 1$, the result of de Gennes is $\bar{Q}(h) \sim -\frac{1}{2}\pi^2 [h/\ln(1-h)]$. For very weak fields, $h \ll 1$, using Eq. (A8), one readily finds

$$\bar{Q}(h) = 1 - \frac{16}{45} h^4, \quad (\text{A11})$$

which should be compared to the result of de Gennes and Meyer in this range, $\bar{Q}(h) = 1 - (\pi^4/512)h^4$. For arbitrary values of h in the range $0 < h < 1$ the quantity $\bar{Q}(h)$ satisfies the equation

$$h \coth(2h/\bar{Q}) + 2(h^2/\bar{Q}) \operatorname{csch}^2(2h/\bar{Q}) = 1. \quad (\text{A12})$$

This equation possesses the noteworthy advantage of analytic simplicity as compared to the pair of equations, (A2) and (A3), which apply when the magnetic energy term is chosen as proportional to $\sin^2\Phi$. In Fig. 7 is shown a plot of $\bar{Q}(h)^{-1}$ vs h for both the treatment by de Gennes as well as for the present approximation. The close numerical agreement of these results leads us to believe that the qualitative nature of the results obtained in the text would be unaffected if one were to employ any of a wide class of periodic functions other than $f(\Phi)$ of Eq. (2.8).

APPENDIX B

We here derive Eq. (2.15) which, when $Ql \leq 1$, provides a very useful expression for the infinite series

$$S(Q, l) = \sum_{n=1}^{\infty} \frac{1}{n} \frac{\tanh(nQl)}{1 + n(Q/\mathcal{C}) \tanh(nQl)}. \quad (\text{B1})$$

We employ the well-known Poisson summation formula⁹ in the form

$$\sum_{n=1}^{\infty} g(n) = -\frac{1}{2}g(0) + \int_0^{\infty} dx g(x) + \sum_{n=1}^{\infty} \int_{-\infty}^{\infty} dx g(x) e^{2\pi i n x}, \quad (\text{B2})$$

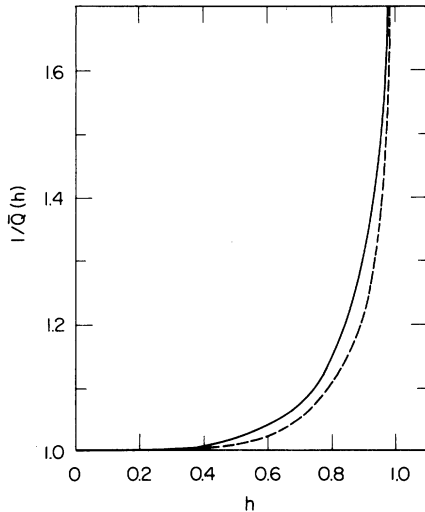


FIG. 7. Plot of the equilibrium pitch in units of the equilibrium pitch for bulk cholesteric vs reduced magnetic field. The dashed curve is the result of de Gennes (Ref. 4) when the magnetic energy term is given by $\frac{1}{2}\chi_a H^2 \sin^2\Phi$. The solid curve is the result when the magnetic energy term is approximated as $(32/\pi^4)\chi_a H^2 \times f(\Phi)$, with $f(\Phi)$ defined by Eq. (2.8). For both curves $1/Q(h)$ increases as h^4 for very small h and as $-\ln(1-h)$ for $h \rightarrow 1-0$.

which is suitable whenever $g(-x) = g(x)$. In the present case we define

$$g(x) = \frac{1}{x} \frac{\tanh(xQl)}{1 + (xQ/\mathcal{C}) \tanh(xQl)} = g(-x). \quad (\text{B3})$$

Now each integral in Eq. (B2) for $n \geq 1$ can be evaluated by utilizing the residue theorem. Specifically, in the upper half of the complex x plane $g(x)$ is analytic with the exception of an infinite set of simple poles which are the zeros of $1 + xQC^{-1} \tanh(xQl)$. These zeros, which are all situated on the positive imaginary axis, will be denoted by iy_m ($m=1, 2, \dots$), and y_m satisfies the equation

$$y_m \tanh y_m = \mathcal{C}l. \quad (\text{B4})$$

The roots of (B4) are ordered so that $y_{m+1} > y_m$. Furthermore, by considering a sequence of concentric semicircles $C(R)$ in the upper half-plane with increasing radii R , carefully selected to avoid the poles at iy_m , one can easily show that the contribution of $\int_{C(R)} dx g(x) e^{2\pi i n x}$ vanishes as $R \rightarrow \infty$. Thus

$$\int_{-\infty}^{\infty} dx g(x) e^{2\pi i n x} = 2\pi i \sum_{m=1}^{\infty} a_{-1}(m) e^{-2\pi n y_m / Ql}, \quad (\text{B5})$$

where $a_{-1}(m)$ denotes the residue of $g(x)$ associated with the simple pole at iy_m . Thus

$$\sum_{n=1}^{\infty} \int_{-\infty}^{\infty} dx g(x) e^{2\pi i n x} = 2\pi i \sum_{m=1}^{\infty} a_{-1}(m) \times \frac{1}{e^{2\pi y_m / Ql} - 1}. \quad (\text{B6})$$

The residues are easily evaluated and the final result is

$$S(Q, l) = A(\mathcal{C}l) - \frac{1}{2}Ql + 2\pi(\mathcal{C}l)^2 \times \sum_{m=1}^{\infty} y_m^{-1} [\exp(2\pi y_m / Ql) - 1]^{-1} \times [\mathcal{C}l + (\mathcal{C}l)^2 + y_m^2]^{-1}, \quad (\text{B7})$$

where

$$A(\mu) = \int_0^{\infty} dx \frac{\tanh x}{x[1 + (x/\mu) \tanh x]}. \quad (\text{B8})$$

The limiting behavior of $A(\mu)$, for values of μ both small and large compared to unity, is readily established. For $\mu \ll 1$, we divide the interval of integration $(0, \infty)$ into the intervals $(0, \beta)$ and (β, ∞) , where β is a constant, small compared to unity, but otherwise arbitrary. Within the interval $(0, \beta)$ the function $\tanh x$ can be replaced by x , and the resulting contribution to $A(\mu)$ is $\frac{1}{2}\pi\mu^{1/2} + O(\mu/\beta)$. The contribution to $A(\mu)$ arising from the

interval (β, ∞) can be written as $\mu \int_{\beta}^{\infty} dx x^{-1} (\tanh x) \times (\mu + x \tanh x)^{-1}$, and the integral remains finite as $\mu \rightarrow 0$. Thus $A(\mu) \sim \frac{1}{2} \pi \mu^{1/2} + O(\mu)$ for $\mu \rightarrow 0$.

For the case $\mu \gg 1$ we write

$$A(\mu) = \int_0^a dx \frac{\tanh x}{x[1 + (x/\mu) \tanh x]} + \int_a^{\infty} dx \frac{1}{x(1 + x/\mu)} + \int_a^{\infty} dx \left(\frac{\tanh x}{1 + (x/\mu) \tanh x} - \frac{1}{1 + (x/\mu)} \right) \frac{1}{x},$$

where a is a positive number, independent of μ , but otherwise arbitrary. Now for large values of μ ,

$$\int_0^a dx \frac{\tanh x}{x[1 + (x/\mu) \tanh x]} \sim \int_0^a dx \frac{\tanh x}{x} + o(1),$$

where the symbol $o(1)$ indicates a term which vanishes as $\mu \rightarrow \infty$. Likewise

$$\int_a^{\infty} dx \left(\frac{\tanh x}{1 + (x/\mu) \tanh x} - \frac{1}{1 + (x/\mu)} \right) \frac{1}{x} \sim - \int_a^{\infty} dx \frac{1 - \tanh x}{x} + o(1)$$

and

$$\int_a^{\infty} dx \frac{1}{x(1 + x/\mu)} = \ln(1 + \mu/a) = \ln \mu - \int_1^a dx \frac{1}{x} + o(1).$$

Combining these terms, for $\mu \rightarrow \infty$, we have

$$A(\mu) \sim \ln \mu + \int_0^1 dx \frac{\tanh x}{x} - \int_1^{\infty} dx \frac{1 - \tanh x}{x} + o(1) \quad (\text{B9})$$

The arbitrary constant a is contained within the term $o(1)$ which vanishes in this limit.

We now show that

$$\int_0^1 dx \frac{\tanh x}{x} - \int_1^{\infty} dx \frac{1 - \tanh x}{x} = \gamma + \ln(4/\pi), \quad (\text{B10})$$

where γ is Euler's constant. The left-hand side of Eq. (B10) can be evaluated by considering the limit $\eta \rightarrow 0$ of the expression¹⁰

$$\int_0^{\infty} dx x^{-1} e^{-\eta x} \tanh x - \int_1^{\infty} dx x^{-1} e^{-\eta x} = \ln(\tfrac{1}{4}\eta) + 2\ln\left(\frac{\Gamma(\tfrac{1}{4}\eta)}{\Gamma(\tfrac{1}{2} + \tfrac{1}{4}\eta)}\right) - E_1(\eta), \quad (\text{B11})$$

where $E_1(\eta)$ is the usual exponential integral function. Utilizing the following properties

$$E_1(\eta) \xrightarrow{\eta \rightarrow 0} -\gamma - \ln \eta + O(\eta), \quad (\text{B12})$$

$$\Gamma(\tfrac{1}{4}\eta)/\Gamma(\tfrac{1}{2} + \tfrac{1}{4}\eta) = 4\pi^{-1/2} \eta^{-1} + O(1),$$

one readily confirms the result in Eq. (B10).

*Present address: Department of Physics, Brookhaven National Laboratory, Upton, New York.

¹F. Rondelez and H. Arnould, C. R. Acad. Sci. B **273**, 549 (1971).

²F. Rondelez and J. P. Hulin, Solid State Commun. **10**, 1009 (1972).

³J. P. Hulin, Appl. Phys. Lett. **21**, 455 (1972).

⁴P. G. de Gennes, Solid State Commun. **6**, 163 (1968). See also R. B. Meyer, Appl. Phys. Lett. **12**, 281 (1968).

⁵An alternate method for measuring C has been proposed by R. B. Meyer, Bull. Am. Phys. Soc. **18**, 40 (1973).

⁶Equation (2.18) is obtained from (2.16) upon replacing $\tanh x$ by $x(1 + \frac{1}{4}x^2)^{-1}$ for $0 < x < 2$ and by unity for $x > 2$.

⁷A. Rapini and M. Papoular, J. Phys. (Paris) Suppl. **30**, 56 (1969).

⁸I. S. Gradshteyn and I. M. Ryzhik, *Tables of Integrals, Series, and Products*, 4th ed. (Academic, New York, 1965), pp. 904-909.

⁹See, for example, P. M. Morse and H. Feshbach, *Methods of Theoretical Physics* (McGraw-Hill, New York, 1953), Part I, pp. 466 and 467.

¹⁰See p. 361, Ref. 8.